Sustainable Energy, Grids and Networks 34 (2023) 101068

Contents lists available at ScienceDirect

Sustainable Energy, Grids and Networks

journal homepage: www.elsevier.com/locate/segan

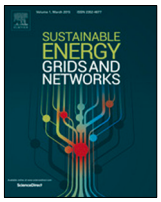

Decentralized coordination between active distribution network and multi-microgrids through a fast decentralized adjustable robust operation framework☆

Xiao Chen [a], Junyi Zhai [b], Yuning Jiang [c,*], Chenyixuan Ni [d], Sheng Wang [e,*], Philippe Nimmegeers [f,g,h]

[a] North China Branch of State Grid Corporation of China, China
[b] College of New Energy, China University of Petroleum (East China), China
[c] Automatic Control Laboratory, École Polytechnique Fédérale de Lausanne (EPFL), Switzerland
[d] Department of Electronic, Electrical and Systems Engineering, University of Birmingham, United Kingdom
[e] State Key Laboratory of the Internet of Things for Smart City, University of Macau, Macau
[f] Intelligence in Processes, Advanced Catalysts and Solvents (iPRACS), Faculty of Applied Engineering, University of Antwerp, Groenenborgerlaan 171, 2020 Antwerp, Belgium
[g] Environmental Economics (EnvEcon), Department of Engineering Management, Faculty of Business and Economics, University of Antwerp, Prinsstraat 13, 2000 Antwerp, Belgium
[h] Flanders Make@UAntwerp, 2000 Antwerp, Belgium

ARTICLE INFO

Article history:
Received 15 May 2022
Received in revised form 10 May 2023
Accepted 14 May 2023
Available online 20 May 2023

Keywords:
Multi-microgrids (MMG)
Adjustable robust optimization
Linear decision rules (LDRs)
Decentralized optimization
Fast alternating direction method of multipliers (ADMM)

ABSTRACT

Due to the autonomous characteristic and heterogeneity of the individual agents in active distribution network (ADN) with multi-microgrids (MMG), this paper proposes a fully decentralized adjustable robust operation framework achieving the coordinated operation between ADN and MMG. The improved linear decision rules (LDRs) based microgrid adjustable robust operation model is proposed to reduce the solution conservatism in dealing with renewable energy uncertainty. The LDRs model is then reformulated as a computationally tractable solution such that the proposed adjustable robust extension of decentralized operation can handle renewable energy uncertainty while reducing the computation burden of decentralized optimization. Then, a tailored fast alternating direction method of multipliers algorithm with a predictor–corrector type acceleration step is developed to improve the convergence rate of decentralized optimization. The effectiveness of the proposed model is validated on a modified IEEE 69-bus distribution system with four microgrids.

1. Introduction

1.1. Background and motivation

To solve global environmental pollution and energy shortages, distributed renewable energy resources such as wind and solar energy have been receiving much attention [1–3]. Microgrids (MGs), with their flexible and efficient integration capabilities, have aroused great attention as an effective way to utilize distributed energy resources as well as become an important part of the active distribution network (ADN) [4,5]. In addition, MGs from different regions can be interconnected to form multi-microgrids (MMG), and each microgrid of MMG could buy/sell power from/to ADN in grid-connected mode. By forming an MMG system, the operational stability and economic efficiency of MGs can be greatly improved. However, it will need to optimize the operation of individual MGs and manage the MMG system of ADN in an integrated manner [6–9]. Therefore, how to effectively coordinate the operation between ADN and MMG has become a hot research topic, which contains two main challenges: (1) the interactive mechanism between ADN and MMG, in which the autonomy and privacy of the distribution system operator and each MG operator needs to be considered; (2) the self-dispatching of MGs, in which intelligent energy management is required to obtain an economical and reliable dispatching scheme considering the uncertainties of renewable energy resources.

☆ This work was supported in part by the Science and Technology Project of State Grid Corporation of China (52010123000M), in part by the Natural Science Foundation of Jiangsu Province (BK20210103), and in part by the Swiss National Science Foundation under the RISK project (200021 175627) and the NCCR Automation (51NF40 180545). Philippe Nimmegeers holds an FWO senior postdoctoral fellowship (1215523N) granted by FWO Vlaanderen/Research Foundation Flanders.

* Corresponding authors.
E-mail addresses: soleilchen@126.com (X. Chen), zhaijunyi@163.com (J. Zhai), yuning.jiang@epfl.ch (Y. Jiang), CXN603@student.bham.ac.uk (C. Ni), wangsheng_zju@zju.edu.cn (S. Wang), philippe.nimmegeers@uantwerpen.be (P. Nimmegeers).

https://doi.org/10.1016/j.segan.2023.101068

Nomenclature

$\mathcal{G}$	Subset of nodes with controllable DGs
$\mathcal{M}$	Set of MGs
$\mathcal{N}$	Set of nodes
$\mathcal{T}$	Set of periods
$\mathcal{U}$	Set of polyhedral uncertainty
ϵ	Maximum deviation of voltage
η^C/η^D	Charging/discharging efficiency of ESS
κ	Uncertainty budget
$\overline{P}^{ex}/\overline{Q}^{ex}$	Exchanged active/reactive power limit between main grid and ADN
$\overline{P}_i^{DN}$	Exchanged active power limit between ADN and MG at node i
$\overline{P}_t^C/\overline{P}_t^D$	Maximum charging/discharging rate of ESS at time t
$\overline{P}_t^W/\overline{P}_t^P$	Predicted output of WT/PV at time t
$\overline{S}_i$	Transmission capacity limit from nodes i to $i+1$
$\underline{E}/\overline{E}$	Minimum/maximum capacity of ESS
$\underline{V}_i/\overline{V}_i$	Minimum/maximum voltage magnitude of node i
$a_i/b_i/c_i$	Fuel cost coefficients of controllable DG i
c^C/c^D	Charging/discharging cost of ESS
c_t^b/c_t^s	Buying/selling price from/to main grid at time t
$P_{i,t}^L$	Load demand of node i at time t
r_i/x_i	Line resistance/reactance between nodes i and $i+1$
R_i^D/R_i^U	Ramp-up/down limit of controllable DG i
$V_{0,t}$	Voltage of substation, normally 1 p.u.
E_t	Actual output of ESS at time t
P_t^b/P_t^s	Active power deficiency/surplus of ADN at time t
P_t^C/P_t^D	Charging/discharging power of ESS at time t
P_t^E	Actual output of ESS at time t
P_t^W/P_t^P	Actual output of WT/PV at time t
$P_t^{MG}/P_{i,t}^{DN}$	Active power injected to MG/flowing from ADN at node i in time t
$P_{1,t}/Q_{1,t}$	Exchanged active/reactive power between main grid and ADN at time t
$P_{i,t}/Q_{i,t}$	Active/reactive power from nodes i to $i+1$ at time t
$P_{i,t}^G/Q_{i,t}^G$	Active/reactive power of controllable DG at node i in time t
$V_{i,t}$	Voltage magnitude of node i at time t

Notation: The main symbols and notation used in the system model are listed here for quick reference. The remaining are defined later when they first appear. Boldface lower case and upper case letters represent vectors and matrices, respectively.

1.2. Literature review

Recently, many studies have been conducted on the coordinated operation problem for ADN with MMG. In [10], a game-theory based method is proposed to simulate the potential cooperative behaviors of MMG to achieve higher energy efficiency and operation economy. In [11], a model predictive control-based dispatching model to maximize the global benefits of MMG is proposed. In [12], a two-stage collaborative operation model for an MMG is constructed, and the interactive energy dispatching model between the distribution network and MMG is addressed in [13]. The dynamic economic dispatch model for the grid-connected and islanded multi-energy microgrids is proposed in [14] to increase the system operating efficiency. An optimal configuration with respect to capacity sizes and types of distributed generators (DGs) for multi-energy microgrids is presented in [15]. The optimal design of microgrids with combined heat and power units is investigated in [16] by coupling environmental and economic sustainability in a multi-objective model. However, the above-mentioned researches are in the way of centralized implementation. When the scale of the ADN or the number of MGs is larger, more information must be collected. The calculation burden will also increase, which may lead to the curse of dimensionality. For centralized implementation, it is also difficult to reflect the different interests of the MGs and the ADN. Nor can the decentralized, autonomous characteristics of a microgrid be described by this kind of model.

Due to the autonomous characteristic and heterogeneity of the individual agents in an active distribution system with multi-microgrids, the distribution system operator and microgrid operator are respectively managed by different entities. Centralized optimization will face technical and political challenges [17–19]. Considering their own benefits, a decentralized framework becomes favorable as it is not always efficient to pool all the local information for centralized computation due to the large size of the problem dimension, a large amount of local data, and privacy issues. In recent years, research on decentralized or distributed energy management for active distribution systems with multi-microgrids has been carried out. The general distributed or decentralized optimization algorithms mainly include alternating direction method of multipliers (ADMM) [20–24], analytical target cascading (ATC) [25,26], Benders decomposition (BD) algorithm [27], heterogeneous decomposition (HD) algorithm [28], and optimality condition decomposition (OCD) [29] algorithm. However, when the number of entities and uncertain renewable energy units is large, the communication burden of HD, OCD, and BD algorithms will be heavy. Thus, the scalability of these methods is not satisfactory [20]. Among them, ADMM has superiority in convergence properties that has been adopted to the integrated transmission-distribution dispatch [21], integrated electricity-gas system operation [22,23], and peer-to-peer energy trading [24] problems.

Another challenge for the operation of a multi-microgrid distribution system is how to hedge uncertainties pertaining to renewable energy. In [30], an energy management scheme based on information gap decision theory is proposed for the energy hub, which can robustly handle uncertainties by defining the interval of objective functions. Considering distribution characteristics for uncertainties, stochastic optimization (SO) has been widely used in the operation of MMGs. A stochastic bi-level operation problem of MMG is presented in [31]. Assuming the driving pattern of electric vehicles to follow chi-square distribution, a two-stage SO integrated energy scheduling strategy for MMG is introduced in [32]. To solve SO problems, scenarios are usually generated based on a probability distribution of uncertain parameters. However, the exact probability distribution in SO is

hard to obtain and SO may pose computational challenges. Differently, as a promising method, robust optimization (RO) [33–43] characterize uncertainties through uncertainty sets and only need their constrained perturbations to find a solution, which is optimal for the worst-case realization. In [41], an adaptive RO with reference distributions is used to confine load demands in MGs. In [42], the risk-averse generation maintenance dispatch for MMG is formulated as a two-stage RO problem. In [43], the RO method is employed to address uncertainties from renewable generation and energy demand for MMG. However, the RO approaches are a decomposition-based master-subproblem iteration algorithm, which may demand a considerable computation time at each iteration. Contrary to the decomposition-based robust approach, the linear decision rules (LDRs) [37–40] model can provide a slightly conservative, yet single-tractable solution to the robust problem. Since the robust counterpart of an LDRs-based adjustable robust approach is usually a tractable convex problem, the LDRs model is more suitable for the application of distributed or decentralized optimization.

Based on the existing research, there are still research gaps that need to be studied.

1. When considering uncertainties in LDRs model for the operatin of active distribution system with multi-microgrids, the existing works [37,38] adopt the allowable output interval to describe uncertainties. However, the adjustable factors of LDRs model must be predefined, which is restrictive and leads to a conservative solution. The other previous works [39,40] adopt the nonadjustable bounded interval to describe uncertainties, which is also quite conservative. Moreover, these LDRs models [37–40] cannot deal with the renewable energy curtailment. As a result, the potential of the LDRs-based adjustable robust model in reducing solution conservatism has not been fully exploited, especially when we consider the renewable energy curtailment and describe uncertainties in a controllable polyhedral uncertainty set.
2. Another alternate to consider uncertainties is the decomposition-based RO models [33–35], which have two disadvantages when deploying distributed ADMM optimization. Firstly, the robust counterpart of the second-stage max–min problem is a bilinear problem. The commonly used outer approximation method or big-M method for this bilinear problem cannot guarantee the convergence of ADMM. Secondly, the calculation burden will be enlarged as the inner master-subproblem iteration of the decomposition-based RO algorithm is needed in each outer ADMM iteration. Therefore, the application of the decomposition-based RO algorithm to the distributed or decentralized operation of active distribution system with multi-microgrids faces many limitations.
3. The widely used distributed ADMM algorithm may converge slowly for solving a distributed convex quadratic programming problem, which requires a large number of iterations to converge. This motivates us to apply a fast ADMM variant to improve the convergence rate of distributed or decentralized optimization. As a result, the applicability of the fast ADMM variant in the distributed operation problem of active distribution system with multi-microgrids should be fully exploited.

1.3. Contribution and organization

To fill the research gap, this paper proposes a fast ADMM-based fully decentralized adjustable robust operation framework for the active distribution system with multi-microgrids, achieving the synergistic yet independent operation of multiple entities. The LDRs-based two-stage adjustable robust approach is adopted to model the highly volatile uncertainties of renewable energies overcoming the disadvantages of the decomposition-based robust approach when applied to decentralized optimization. The contributions of this paper are summarized as follows:

1. A fully decentralized coordinated operation framework for the active distribution system with multi-microgrids is proposed, achieving the synergistic yet independent operation of multiple entities. Then, a tailored fast ADMM algorithm, which is an accelerated variant of standard ADMM with a predictor–corrector type acceleration step, is proposed. Compared with the standard ADMM, the proposed fast ADMM approach has one more restarting step, which can improve the convergence of decentralized optimization.
2. An improved LDRs model is proposed for the robust operation of MMG. Compared to the works in [37,38] that regard the adjustable factors of the LDRs model as constants, we regard the adjustable factors as variables. Compared to the works in [39,40] that describe uncertainties in the LDRs model through non-adjustable intervals, we adopt a controllable polyhedral uncertainty set to control the solution conservatism. Meanwhile, renewable energy curtailment can be handled. As a result, the proposed LDRs model for the robust operation of MMG can simultaneously consider the renewable energy curtailment, optimize the adjustable factors, and utilize the budget of uncertainty in a polyhedral uncertainty set.
3. The LDRs-based adjustable robust extension of fast ADMM-based decentralized framework capable of handling renewable uncertainties in active distribution system with multi-microgrids is proposed. LDRs are utilized to recast the microgrid adjustable robust problem into a single tractable convex problem, which can reduce the computation burden of each fast ADMM iteration and guarantee its convergence. Meanwhile, by aggregating the uncertainties, only a one-dimensional random variable needs to be considered rather than a high-dimensional random variable. Therefore, the computation burden of the LDRs model does not increase with the number of uncertain sources.

The rest of this paper is organized as follows. The separable formulation of the deterministic operation model is introduced in Section 2. The compact LDRs-based microgrid adjustable robust operation model is presented in Section 3. The decentralized adjustable robust operation framework is summarized in Section 4. Section 5 presents the numerical results and conclusions are given in Section 6.

2. Separable formulation of deterministic operation model

This section introduces the affinely coupled separable formulation of the deterministic operation model for the multi-microgrids distribution system amenable to decentralized optimization.

2.1. Topology of distribution system with multi-microgrids

A typical topology of the multi-microgrids distribution system is shown in Fig. 1. The microgrid organically combines the photovoltaic (PV), wind turbine (WT), and energy storage system (ESS) to meet the local load demand. When the MMG generation is excessive or insufficient, the MMG will exchange power flow with ADN. Similarly, the ADN satisfies its own load demand with the controllable DGs and coordinates the power transmission with the main grid.

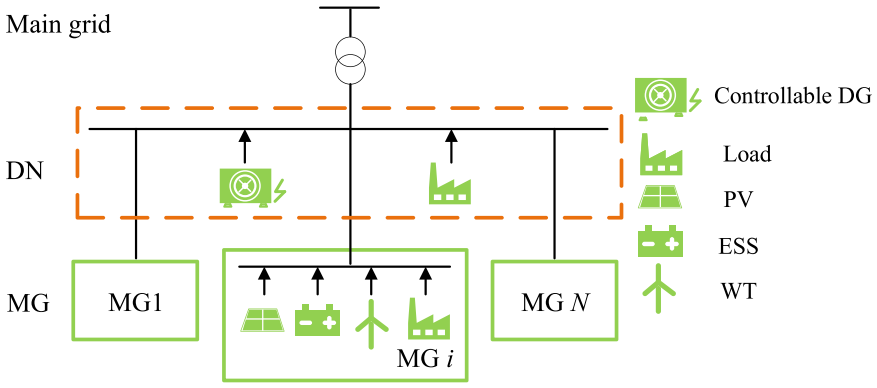

Fig. 1. Topology of distribution system with multi-microgrids.

2.2. Operation problem of ADN

The optimization objective of ADN is to minimize the operation costs of controllable DGs as well as the power transaction costs including electricity purchasing costs or selling benefits from the main grid. By considering a buying price higher than the selling price, we can promote the self-consumption of ADN over exporting power to the main grid. The corresponding optimization model is formulated as follows:

$$\min \sum_{t\in\mathcal{T}}\sum_{i\in\mathcal{G}}\left[a_i\left(P_{i,t}^{G}\right)^2+b_iP_{i,t}^{G}+c_i\right]+\sum_{t\in\mathcal{T}}\left(c_t^bP_t^b-c_t^sP_t^s\right) \tag{1a}$$

$$\text{subject to}\quad P_{i+1,t}=P_{i,t}+P_{i+1,t}^{G}-P_{i+1,t}^{L}-P_{i+1,t}^{DN},\ i\in\mathcal{N},\ t\in\mathcal{T} \tag{1b}$$

$$Q_{i+1,t}=Q_{i,t}+Q_{i+1,t}^{G}-Q_{i+1,t}^{L},\ i\in\mathcal{N},\ t\in\mathcal{T} \tag{1c}$$

$$V_{i+1,t}=V_{i,t}-\frac{r_iP_{i,t}+x_iQ_{i,t}}{V_{0,t}},\ i\in\mathcal{N},\ t\in\mathcal{T} \tag{1d}$$

$$P_{1,t}=P_t^b-P_t^s,\ P_t^b\geq 0,\ P_t^s\geq 0,\ t\in\mathcal{T} \tag{1e}$$

$$-\overline{P}^{ex}\leq P_{1,t}\leq\overline{P}^{ex},\ t\in\mathcal{T} \tag{1f}$$

$$-\overline{Q}^{ex}\leq Q_{1,t}\leq\overline{Q}^{ex},\ t\in\mathcal{T} \tag{1g}$$

$$P_{i,t}^2+Q_{i,t}^2\leq\overline{S}_i^2,\ i\in\mathcal{N},\ t\in\mathcal{T} \tag{1h}$$

$$1-\epsilon\leq V_{i,t}\leq 1+\epsilon,\ i\in\mathcal{N},\ t\in\mathcal{T} \tag{1i}$$

$$-\overline{P}_i^{DN}\leq P_{i,t}^{DN}\leq\overline{P}_i^{DN},\ i\in\mathcal{M},\ t\in\mathcal{T} \tag{1j}$$

$$\underline{P}_i^{G}\leq P_{i,t}^{G}\leq\overline{P}_i^{G},\ i\in\mathcal{G},\ t\in\mathcal{T} \tag{1k}$$

$$-R_i^{D}\leq P_{i,t}^{G}-P_{i,t-1}^{G}\leq R_i^{U},\ i\in\mathcal{G},\ t\in\mathcal{T} \tag{1l}$$

$$\underline{Q}_i^{G}\leq Q_{i,t}^{G}\leq\overline{Q}_i^{G},\ i\in\mathcal{G},\ t\in\mathcal{T}. \tag{1m}$$

The objective (1a) minimizes the total operation costs of ADN. Constraints (1b)–(1d) are the linearized distribution load flow (Dist-Flow) equations. The Dist-Flow model is originally proposed in [44] and linearized in [45]. The linearized DistFlow branch model is more appropriate than the DC power flow model by incorporating reactive power and voltage magnitudes, as it can produce a solution, which is comparable with the classical DistFlow branch model. Constraints (1e)–(1g) represent the relationship between the power flow from the main grid to the ADN. It is noted that $P_t^b>0$ means the ADN buys electricity from the main grid and $P_t^s>0$ means the ADN sells electricity to the main grid. Constraint (1h) denotes the branch capacity limit. Constraint (1i) ensures the voltage magnitude of each node is kept within the allowed maximum deviation from the nominal value. Constraint (1j) denotes the power flow limits transferred from ADN to MMG. Constraints (1k)–(1m) are the generation limits on controllable DGs.

For the quadratic constraint (1h), we propose a number of linear constraints (2) to substitute it. Intuitively speaking, this procedure is approximating the original circular feasible region using an octagon.

$$-\overline{S}_i\leq P_{i,t}\leq\overline{S}_i, \tag{2a}$$

$$-\overline{S}_i\leq Q_{i,t}\leq\overline{S}_i, \tag{2b}$$

$$-\sqrt{2}\overline{S}_i\leq P_{i,t}+Q_{i,t}\leq\sqrt{2}\overline{S}_i, \tag{2c}$$

$$-\sqrt{2}\overline{S}_i\leq P_{i,t}-Q_{i,t}\leq\sqrt{2}\overline{S}_i. \tag{2d}$$

2.3. Operation problem of MMG

The optimization objective of MMG aims for the minimum operation cost of ESS. The operation model of the kth MG (omitting the subscript k in further notation) is written as:

$$\min \sum_{t\in\mathcal{T}}\left(c^CP_t^C+c^DP_t^D\right) \tag{3a}$$

$$\text{subject to}\quad P_t^W+P_t^P+P_t^D-P_t^C+P_t^{MG}=P_t^L,\ t\in\mathcal{T} \tag{3b}$$

$$-\overline{P}^{DN}\leq P_t^{MG}\leq\overline{P}^{DN},\ t\in\mathcal{T} \tag{3c}$$

$$0\leq P_t^W\leq\overline{P}_t^W,\ t\in\mathcal{T} \tag{3d}$$

$$0\leq P_t^P\leq\overline{P}_t^P,\ t\in\mathcal{T} \tag{3e}$$

$$0\leq P_t^C\leq\overline{P}^C,\ t\in\mathcal{T} \tag{3f}$$

$$0\leq P_t^D\leq\overline{P}^D,\ t\in\mathcal{T} \tag{3g}$$

$$E_t=E_{t-1}+\eta^CP_t^C\Delta t-P_t^D\Delta t/\eta^D,\ t\in\mathcal{T} \tag{3h}$$

$$\underline{E}\leq E_t\leq\overline{E},\ t\in\mathcal{T} \tag{3i}$$

$$E_0=E_T. \tag{3j}$$

The objective function (3a) minimizes the total operation costs of each MG. Here, note that reactive power transmission between the ADN and MMG is not considered in this paper. Constraint (3b) represents the power balance of MG while constraint (3c) denotes the power flow limits transferred from the MG to the ADN. Constraints (3d) and (3e) is the power production limit for WT and PV, respectively. Constraints (3f)–(3g) denote the charging and discharging rate limits of ESS [46]. Constraint (3h) represents the energy balance of ESS. Constraint (3i) keeps the energy of ESS within its capacity limits. Constraint (3j) specifies the initial and final energy level of ESS. Note that the operation cost function of ESS in (3a) and the charging/discharging efficiency will lead to extra energy loss and energy cost in the case of simultaneous charge/discharge, the case of simultaneous charge/discharge will never happen in an optimal energy schedule for ESS.

Remark 1. Model (3) can avoid simultaneous charging and discharging of ESS without introducing binary variables. To further explain this point, we simplify constraint (3b) as

$$P_t^D - P_t^C = \Delta P_t^{CD},\ t \in \mathcal{T} \quad \text{with} \quad \Delta P_t^{CD} = P_t^L - P_t^W - P_t^P - P_t^{MG}.$$

Then, we can simplify the objective (3a) as:

$$\min \quad \sum_{t\in\mathcal{T}} \left((c^C + c^D)P_t^C + c^D \Delta P_t^{CD}\right) \quad \text{with} \quad P_t^C \in [0, \overline{P}^C], \tag{4a}$$

or

$$\min \quad \sum_{t\in\mathcal{T}} \left((c^C + c^D)P_t^D - c^D \Delta P_t^{CD}\right) \quad \text{with} \quad P_t^D \in [0, \overline{P}^D]. \tag{4b}$$

Due to $c^C, c^D > 0$, it is clear that the objective (4a) and objective (4b) monotonic increasing with respect to P_t^C and P_t^D, respectively. Therefore, we have either the charging power $P_t^C = 0$ or discharging $P_t^D = 0$.

2.4. Coupling of ADN and MMG

Area coupling constraints tend to guarantee the agreement on tie-line power between ADN and MMG. While implementing the decentralized optimization, it is necessary that the output power from the ADN should be equal to the input power to the MMG. Hence, the area coupling constraint (5) should be established.

$$P_{k,t}^{DN} = P_{k,t}^{MG},\ k \in \mathcal{M},\ t \in \mathcal{T}. \tag{5}$$

The operation problem for each MG is an independent decision-making process that does not contain information about other neighboring MGs. Namely, there is no information exchange among MGs. Only tie-line information is shared between ADN and MMG to ensure consistency in operation. Therefore, the coordinated operation problem of a multi-microgrids distribution system can be solved in a fully decentralized way, preserving the independent decision of each subsystem operator.

3. Compact LDRs-based microgrid adjustable robust operation model

This section introduces the main idea of the LDRs-based adjustable operation model for MGs using a compact form. The robust adjustable model includes two stages, i.e., "here-and-now" and "wait-and-see". Each MG negotiates with the ADN to obtain their coordinated "here-and-now" decisions prior to the uncertainty realizations at the first stage. Then, each MG takes local "wait-and-see" recourse decisions that compensate the forecast deviations in real-time to keep the negotiated tie-line power constant at the second stage.

For the sake of presentation, we write the deterministic operation model of each MG into the following compact epigraph form:

$$\min_{\boldsymbol{x},\boldsymbol{y}} \quad \Phi(\boldsymbol{x}, \boldsymbol{y}) \tag{6a}$$

$$\text{subject to} \quad \boldsymbol{A}\cdot\boldsymbol{x} + \boldsymbol{B}\cdot\boldsymbol{y} + \boldsymbol{C}\cdot\hat{\boldsymbol{\xi}} + \boldsymbol{e} = 0, \tag{6b}$$

$$\boldsymbol{D}\cdot\boldsymbol{x} + \boldsymbol{E}\cdot\boldsymbol{y} + \boldsymbol{F}\cdot\hat{\boldsymbol{\xi}} + \boldsymbol{f} \le 0 \tag{6c}$$

with coefficient matrices $\boldsymbol{A}$, $\boldsymbol{B}$, $\boldsymbol{C}$, $\boldsymbol{D}$, $\boldsymbol{E}$, and $\boldsymbol{F}$ in appropriate dimensions, $\boldsymbol{e}, \boldsymbol{f}$ denote the requirement vectors, $\boldsymbol{x}$ denotes the "here-and-now" variables made before the realization of uncertainty, variables $\boldsymbol{y}$ can take "wait-and-see" recourse decisions, function $\Phi(\cdot,\cdot)$ denotes the compact linear objective, $\hat{\boldsymbol{\xi}}$ denotes a forecast value of the uncertainty of renewable energy denoted by vector $\boldsymbol{\xi}$.

In this paper, the uncertain parameter $\boldsymbol{\xi}$ is restricted by being in a polyhedral uncertainty set given by

$$\mathcal{U} = \{\boldsymbol{\xi} \ge 0,\ \boldsymbol{K}\cdot\boldsymbol{\xi} - \boldsymbol{g} \le 0\}. \tag{7}$$

The robustness level can be controlled using a parameter denominated as the budget of uncertainty. The robust form of (6c) can be, thus, written as the following semi-infinite form:

$$\forall\, \boldsymbol{\xi} \in \mathcal{U},\ \ \boldsymbol{D}\cdot\boldsymbol{x} + \boldsymbol{E}\cdot\boldsymbol{y} + \boldsymbol{F}\cdot\boldsymbol{\xi} + \boldsymbol{f} \le 0, \tag{8}$$

which ensures the robustness of the optimal solution against any realization of uncertain parameters.

The decision variable $\boldsymbol{y}$ is replaced by an LDR including two parts,

$$\boldsymbol{y} = \boldsymbol{y}^{\mathrm{N}} + \boldsymbol{y}^{\mathrm{A}}\cdot\boldsymbol{\xi}, \tag{9}$$

where non-adjustable variable $\boldsymbol{y}^{\mathrm{N}}$ is the "here-and-now" part made before the realization of uncertainty. Adjustable variable $\boldsymbol{y}^{\mathrm{A}}$ is the "wait-and-see" part made after the uncertain parameters are revealed, which can be regarded as the adjustable factors of controllable DGs.

Thus, (8) can be further rewritten as

$$\forall\, \boldsymbol{\xi} \in \mathcal{U},\ \ \boldsymbol{D}\cdot\boldsymbol{x} + \boldsymbol{E}\cdot\left(\boldsymbol{y}^{\mathrm{N}} + \boldsymbol{y}^{\mathrm{A}}\cdot\boldsymbol{\xi}\right) + \boldsymbol{F}\cdot\boldsymbol{\xi} + \boldsymbol{f} \le 0. \tag{10}$$

The constraint (10) is feasible for any realization of the uncertain parameters if it is feasible for the worst-case realization of the uncertain parameters such that (10) is equivalent to

$$\max_{\boldsymbol{\xi}\in\mathcal{U}} \quad \left\{\boldsymbol{E}\cdot\left(\boldsymbol{y}^{\mathrm{N}} + \boldsymbol{y}^{\mathrm{A}}\cdot\boldsymbol{\xi}\right) + \boldsymbol{F}\cdot\boldsymbol{\xi}\right\} + \boldsymbol{D}\cdot\boldsymbol{x} + \boldsymbol{f} \le 0. \tag{11}$$

The worst-case constraint (11) can be further simplified by using duality theory [47] to eliminate the max operator such that the robust form of (6) is given by

$$\min_{\boldsymbol{x},\boldsymbol{y}^{\mathrm{N}},\boldsymbol{y}^{\mathrm{A}},\boldsymbol{\Lambda},\boldsymbol{\Pi}} \quad \overline{\Phi}\left(\boldsymbol{x}, \boldsymbol{y}^{\mathrm{N}}, \boldsymbol{y}^{\mathrm{A}}, \boldsymbol{\Lambda}\right) \tag{12a}$$

$$\text{subject to} \quad \boldsymbol{A}\cdot\boldsymbol{x} + \boldsymbol{B}\cdot\boldsymbol{y}^{\mathrm{N}} + \boldsymbol{C}\cdot\hat{\boldsymbol{\xi}} + \boldsymbol{e} = 0 \tag{12b}$$

$$\boldsymbol{D}\cdot\boldsymbol{x} + \boldsymbol{E}\cdot\boldsymbol{y}^{\mathrm{N}} + \boldsymbol{\Pi}^{\top}\cdot\boldsymbol{g} + \boldsymbol{f} \le 0 \tag{12c}$$

$$\boldsymbol{\Pi}^{\top}\cdot\boldsymbol{K} \ge \boldsymbol{E}\cdot\boldsymbol{y}^{\mathrm{A}} + \boldsymbol{F} \tag{12d}$$

$$\boldsymbol{\Lambda},\ \boldsymbol{\Pi} \ge 0 \tag{12e}$$

with associated dual variable $\boldsymbol{\Lambda}$ and $\boldsymbol{\Pi}$.

Here, the reformulation of the worst-case objective is the same as the reformulation of constraints (11) by using the duality theory such that $\overline{\Phi}$ is also linear [48]. Accordingly, the resulting adjustable robust operation model (12) is a tractable LP problem, which can be efficiently and directly solved by off-the-shelf optimization packages, e.g., `Gurobi`. Moreover, the above LDRs-based adjustable robust model can simultaneously consider the renewable energy curtailment, optimize the adjustable factors of controllable DGs, and utilize the budget of uncertainty in a polyhedral uncertainty set to reduce the conservatism of robust solutions. The extended formulation of the LDRs model can be seen in Appendix.

4. Fast ADMM-based fully decentralized adjustable robust operation framework

This section proposes a fast ADMM-based fully decentralized adjustable robust operation formulation for the distribution system based multi-microgrids. To this end, we first stack by $\boldsymbol{\chi}_0$ and $\boldsymbol{\chi}_a$, $a \in \mathcal{R}$ the local decision variables of the ADN and the ath sub-MG. Here, $\mathcal{R}$ denotes the index of local systems including the ADN and MMG. Following the star-topology described in Fig. 1, i.e., all MGs are connected with ADN but not connected with each other, we can now rewrite the adjustable robust operation model for ADN with MMG as the following distributed convex quadratic form

$$\min_{\chi} \quad \Psi_0(\boldsymbol{\chi}_0) + \sum_{a\in\mathcal{R}} \Psi_a(\boldsymbol{\chi}_a) \tag{13a}$$

$$\text{subject to} \quad \boldsymbol{\Gamma}_{0,a}\boldsymbol{\chi}_0 = \boldsymbol{\Gamma}_{a,0}\boldsymbol{\chi}_a,\ a \in \mathcal{R} \tag{13b}$$

$$\boldsymbol{\chi}_0 \in \mathcal{X}_0,\ \boldsymbol{\chi}_a \in \mathcal{X}_a,\ a \in \mathcal{R} \tag{13c}$$

with convex quadratic objective Ψ_0, and decoupled linear objective Ψ_a for all $a \in \mathcal{R}$. Local constraint sets $\mathcal{X}_0$, $\mathcal{X}_a$, $a \in \mathcal{R}$ collects all decoupled constraints and their associated robust tractable reformulation introduced in Sections 2 and 3 for the ADN and each MG, respectively. Here, the coupled affine equality constraint (13b) summarizes constraints (5) for all $a \in \mathcal{R}$ with selection matrices $\Gamma_{a,0}$ and $\Gamma_{0,a}$.

In order to solve (13) using ADMM in a fully decentralized manner, we introduce consensus variables $\boldsymbol{\zeta}$ with the following affine equalities

$$\boldsymbol{\Gamma}_{0,a}\boldsymbol{\chi}_0 = \boldsymbol{\zeta}_{0,a},\ \boldsymbol{\Gamma}_{a,0}\boldsymbol{\chi}_a = \boldsymbol{\zeta}_{0,a},\ a \in \mathcal{R} \tag{14}$$

where the auxiliary decision variables $\boldsymbol{\zeta}_{0,a}$ introduces the indirect coupling between ADN and ath MG.

As a result, the augmented Lagrangian is written as

$$L(\boldsymbol{\chi}, \boldsymbol{\zeta}, \boldsymbol{\lambda}) := \Psi_0(\chi_0) + \sum_{a\in\mathcal{R}} \left\{ \Psi_a(\boldsymbol{\chi}_a) + \begin{bmatrix}\boldsymbol{\lambda}_{0,a}\\ \boldsymbol{\lambda}_{a,0}\end{bmatrix}^\top \begin{bmatrix}\boldsymbol{\Gamma}_{0,a}\boldsymbol{\chi}_0 - \boldsymbol{\zeta}_{0,a}\\ \boldsymbol{\Gamma}_{a,0}\boldsymbol{\chi}_a - \boldsymbol{\zeta}_{0,a}\end{bmatrix} + \frac{\rho}{2}\left\| \begin{bmatrix}\boldsymbol{\Gamma}_{0,a}\boldsymbol{\chi}_0 - \boldsymbol{\zeta}_{0,a}\\ \boldsymbol{\Gamma}_{a,0}\boldsymbol{\chi}_a - \boldsymbol{\zeta}_{0,a}\end{bmatrix}\right\|_2^2 \right\},$$

where $\boldsymbol{\lambda}_{0,a}$ and $\boldsymbol{\lambda}_{a,0}$ denotes the Lagrangian multipliers of (14), ρ is the penalty parameter. The standard ADMM iteration is thus outlined as follows.

Algorithm 1: Standard ADMM for Solving (13)

Input : $(\boldsymbol{\zeta}^0_{0,a},\ \boldsymbol{\lambda}^0_{0,a},\ \boldsymbol{\lambda}^0_{a,0}),\ a \in \mathcal{R},\ \rho > 0$

For ℓ =0, 1, 2, 3, ...

$$\boldsymbol{\chi}_0^{\ell+1} = \underset{\boldsymbol{\chi}_0\in\mathcal{X}_0}{\operatorname{argmin}}\ \Psi_0(\boldsymbol{\chi}_0) + \sum_{a\in\mathcal{R}} \left((\boldsymbol{\Gamma}_{0,a}\boldsymbol{\chi}_0)^\top \boldsymbol{\lambda}^\ell_{0,a} + \frac{\rho}{2}\left\| \boldsymbol{\Gamma}_{0,a}\boldsymbol{\chi}_0 - \boldsymbol{\zeta}^\ell_{0,a}\right\|_2^2 \right) \tag{15a}$$

$$\boldsymbol{\chi}_a^{\ell+1} = \underset{\boldsymbol{\chi}_a\in\mathcal{X}_a}{\operatorname{argmin}}\ \Psi_a(\boldsymbol{\chi}_a) + (\boldsymbol{\Gamma}_{a,0}\boldsymbol{\chi}_a)^\top \boldsymbol{\lambda}^\ell_{a,0} + \frac{\rho}{2}\left\| \boldsymbol{\Gamma}_{a,0}\boldsymbol{\chi}_a - \boldsymbol{\zeta}^\ell_{0,a}\right\|_2^2,\ a \in \mathcal{R} \tag{15b}$$

$$\boldsymbol{\zeta}_{0,a}^{\ell+1} = \underset{\boldsymbol{\zeta}_{0,a}}{\operatorname{argmin}} \begin{bmatrix}\boldsymbol{\lambda}^\ell_{0,a}\\ \boldsymbol{\lambda}^\ell_{a,0}\end{bmatrix}^\top \begin{bmatrix}\boldsymbol{\Gamma}_{0,a}\boldsymbol{\chi}_0^{\ell+1} - \boldsymbol{\zeta}_{0,a}\\ \boldsymbol{\Gamma}_{a,0}\boldsymbol{\chi}_a^{\ell+1} - \boldsymbol{\zeta}_{0,a}\end{bmatrix} + \frac{\rho}{2}\left\| \begin{bmatrix}\boldsymbol{\Gamma}_{0,a}\boldsymbol{\chi}_0^{\ell+1} - \boldsymbol{\zeta}_{0,a}\\ \boldsymbol{\Gamma}_{a,0}\boldsymbol{\chi}_a^{\ell+1} - \boldsymbol{\zeta}_{0,a}\end{bmatrix}\right\|_2^2 = \frac{\boldsymbol{\lambda}^\ell_{a,0} + \boldsymbol{\lambda}^\ell_{0,a}}{2} + \frac{\rho(\boldsymbol{\Gamma}_{0,a}\boldsymbol{\chi}_0^{\ell+1} + \boldsymbol{\Gamma}_{a,0}\boldsymbol{\chi}_a^{\ell+1})}{2},\ a \in \mathcal{R} \tag{15c}$$

$$\boldsymbol{\lambda}^{\ell+1}_{0,a} = \boldsymbol{\lambda}^\ell_{0,a} + \rho(\boldsymbol{\Gamma}_{0,a}\boldsymbol{\chi}_0^{\ell+1} - \boldsymbol{\zeta}^{\ell+1}_{0,a}),\ a \in \mathcal{R} \tag{15d}$$

$$\boldsymbol{\lambda}^{\ell+1}_{a,0} = \boldsymbol{\lambda}^\ell_{a,0} + \rho(\boldsymbol{\Gamma}_{a,0}\boldsymbol{\chi}_a^{\ell+1} - \boldsymbol{\zeta}^{\ell+1}_{a,0}),\ a \in \mathcal{R} \tag{15e}$$

End for

Here, ℓ denotes a global iteration counter. The local primal update (15a) and (15b) can be deployed in parallel. Then, the explicit update of $\boldsymbol{\zeta}_{0,a}$ and dual pair $(\boldsymbol{\lambda}_{0,a}, \boldsymbol{\lambda}_{a,0})$ can be sequentially calculated in parallel at the local MG's computational unit. Algorithm 1 only requires one forward–backward communication round between the ADN and MMG. However, as literature, e.g., [49], illustrated, in practice, the standard ADMM converges slowly for solving a distributed convex quadratic programming. To improve its convergence speed, we propose a fast ADMM approach to deal with (13) as follows.

Algorithm 2: Fast ADMM with Restart for Solving (13)

Input : $(\boldsymbol{\zeta}^0_{0,a} = \hat{\boldsymbol{\zeta}}^1_{0,a},\ \boldsymbol{\lambda}^0_{0,a} = \hat{\boldsymbol{\lambda}}^1_{0,a},\ \boldsymbol{\lambda}^0_{a,0} = \hat{\boldsymbol{\lambda}}^1_{a,0}),\ a \in \mathcal{R},\ \rho > 0,\ \theta^0 > 0,\ \beta \in (0,1),\ \sigma^0 = 1$

For ℓ =1, 2, 3, ...

$$\boldsymbol{\chi}_0^{\ell} = \underset{\boldsymbol{\chi}_0\in\mathcal{X}_0}{\operatorname{argmin}}\ \Psi_0(\boldsymbol{\chi}_0) + \sum_{a\in\mathcal{R}} \left((\boldsymbol{\Gamma}_{0,a}\boldsymbol{\chi}_0)^\top \hat{\boldsymbol{\lambda}}^\ell_{0,a} + \frac{\rho}{2}\left\| \boldsymbol{\Gamma}_{0,a}\boldsymbol{\chi}_0 - \hat{\boldsymbol{\zeta}}^\ell_{0,a}\right\|_2^2 \right) \tag{16a}$$

$$\boldsymbol{\chi}_a^{\ell} = \underset{\boldsymbol{\chi}_a\in\mathcal{X}_a}{\operatorname{argmin}}\ \Psi_a(\boldsymbol{\chi}_a) + (\boldsymbol{\Gamma}_{a,0}\boldsymbol{\chi}_a)^\top \hat{\boldsymbol{\lambda}}^\ell_{a,0} + \frac{\rho}{2}\left\| \boldsymbol{\Gamma}_{a,0}\boldsymbol{\chi}_a - \boldsymbol{\zeta}^\ell_{0,a}\right\|_2^2,\ a \in \mathcal{R}$$

$$\boldsymbol{\zeta}_{0,a}^{\ell} = \underset{\boldsymbol{\zeta}_{0,a}}{\operatorname{argmin}} \begin{bmatrix}\hat{\boldsymbol{\lambda}}^\ell_{0,a}\\ \hat{\boldsymbol{\lambda}}^\ell_{a,0}\end{bmatrix}^\top \begin{bmatrix}\boldsymbol{\Gamma}_{0,a}\boldsymbol{\chi}_0^{\ell} - \boldsymbol{\zeta}_{0,a}\\ \boldsymbol{\Gamma}_{a,0}\boldsymbol{\chi}_a^{\ell} - \boldsymbol{\zeta}_{0,a}\end{bmatrix} + \frac{\rho}{2}\left\| \begin{bmatrix}\boldsymbol{\Gamma}_{0,a}\boldsymbol{\chi}_0^{\ell} - \boldsymbol{\zeta}_{0,a}\\ \boldsymbol{\Gamma}_{a,0}\boldsymbol{\chi}_a^{\ell} - \boldsymbol{\zeta}_{0,a}\end{bmatrix}\right\|_2^2 \tag{16b}$$

$$= \frac{\hat{\boldsymbol{\lambda}}^\ell_{a,0} + \hat{\boldsymbol{\lambda}}^\ell_{0,a}}{2} + \frac{\rho(\boldsymbol{\Gamma}_{0,a}\boldsymbol{\chi}_0^{\ell} + \boldsymbol{\Gamma}_{a,0}\boldsymbol{\chi}_a^{\ell})}{2},\ a \in \mathcal{R} \tag{16c}$$

$$\boldsymbol{\lambda}^{\ell}_{0,a} = \hat{\boldsymbol{\lambda}}^\ell_{0,a} + \rho(\boldsymbol{\Gamma}_{0,a}\boldsymbol{\chi}_0^{\ell} - \boldsymbol{\zeta}^{\ell}_{0,a}),\ a \in \mathcal{R} \tag{16d}$$

$$\boldsymbol{\lambda}^{\ell}_{a,0} = \hat{\boldsymbol{\lambda}}^\ell_{a,0} + \rho(\boldsymbol{\Gamma}_{a,0}\boldsymbol{\chi}_a^{\ell} - \boldsymbol{\zeta}^{\ell}_{a,0}),\ a \in \mathcal{R} \tag{16e}$$

if $\theta^\ell = \sum_{a\in\mathcal{R}} \rho^{-1} \left\| \begin{bmatrix}\boldsymbol{\lambda}^\ell_{0,a} - \boldsymbol{\lambda}^\ell_{0,a}\\ \boldsymbol{\lambda}^\ell_{a,0} - \boldsymbol{\lambda}^\ell_{a,0}\end{bmatrix}\right\|_2^2 + \rho \left\| \boldsymbol{\zeta}^\ell_{0,a} - \boldsymbol{\zeta}^\ell_{0,a}\right\|_2^2 < \beta \cdot \theta^{\ell-1}$ (16f)

$$\sigma^{\ell+1} = \frac{1 + \sqrt{1 + 4(\sigma^\ell)^2}}{2} \tag{16g}$$

$$\hat{\boldsymbol{\lambda}}^{\ell+1}_{0,a} = \boldsymbol{\lambda}^{\ell+1}_{0,a} + \frac{\sigma^\ell - 1}{\sigma^{\ell+1}}(\boldsymbol{\lambda}^{\ell+1}_{0,a} - \boldsymbol{\lambda}^{\ell}_{0,a}),\ a \in \mathcal{R} \tag{16h}$$

$$\hat{\boldsymbol{\lambda}}^{\ell+1}_{a,0} = \boldsymbol{\lambda}^{\ell+1}_{a,0} + \frac{\sigma^\ell - 1}{\sigma^{\ell+1}}(\boldsymbol{\lambda}^{\ell+1}_{a,0} - \boldsymbol{\lambda}^{\ell}_{a,0}),\ a \in \mathcal{R} \tag{16i}$$

$$\hat{\boldsymbol{\zeta}}^{\ell+1}_{0,a} = \boldsymbol{\zeta}^{\ell+1}_{0,a} + \frac{\sigma^\ell - 1}{\sigma^{\ell+1}}(\boldsymbol{\zeta}^{\ell+1}_{0,a} - \boldsymbol{\zeta}^{\ell}_{0,a}),\ a \in \mathcal{R} \tag{16j}$$

else

$$\sigma^{\ell+1} = 1,\ \hat{\boldsymbol{\lambda}}^{\ell+1}_{0,a} = \boldsymbol{\lambda}^{\ell}_{0,a},\ \hat{\boldsymbol{\lambda}}^{\ell+1}_{a,0} = \boldsymbol{\lambda}^{\ell}_{a,0},\ \hat{\boldsymbol{\zeta}}^{\ell+1}_{0,a} = \boldsymbol{\zeta}^{\ell}_{0,a},\ a \in \mathcal{R} \tag{16k}$$

End

End for

Compared to Algorithm 1, Algorithm 2 uses a predictor–corrector type acceleration strategy, i.e., steps (16g)–(16j), to improve the convergence performance. The main idea is to deploy Nesterov's acceleration [50] to update $\hat{\boldsymbol{\zeta}}_{0,a}$ and $(\hat{\boldsymbol{\lambda}}_{0,a}, \hat{\boldsymbol{\lambda}}_{a,0})$ for all $a \in \mathcal{R}$. However, the acceleration step is stable only when the objectives Ψ_0, Ψ_a for all $a \in \mathcal{R}$ are strongly convex such that a restarting strategy has to be implemented for generic convergence guarantee [51]. In Algorithm 2, the restating step (16f) implements the acceleration when the residual θ^ℓ is decreased. Otherwise, the iterations of Algorithm 2 are equivalent to Algorithm 1.

Remark 2 (*Convergence Rate*)**.** When all Ψ_a and Ψ_0 are strongly convex, [51] has shown that Algorithm 2 without the restarting can improve the convergence rate from the standard ADMM's $\mathcal{O}(\frac{1}{\ell})$ to $\mathcal{O}(\frac{1}{\ell^2})$. Unfortunately, our problem (13) does not satisfy this assumption, which can only achieve convergence guarantee [52] by deploying the restarting step but without a convergence rate. In practice, some heuristic regularization tricks can be used to enforce the strong convexity of the objective [53], but

Table 1
Comparison of different uncertainty budgets with 12 step size.

κ	Total operation cost ($)			Computation time (s)
	Case 1	Case 2	Case 3	
0	1980.41	1980.41	1980.41	1.03
12	2085.74	2207.26	2340.33	1.62
24	2085.74	2207.26	2340.33	1.65
36	2085.74	2207.26	2340.33	1.97
48	2085.74	2207.26	2340.33	1.74

Table 2
Comparison of different uncertainty budgets with 0.05 step size.

κ	Total operation cost ($)			Computation time (s)
	Case 1	Case 2	Case 3	
0	1980.41	1980.41	1980.41	1.03
0.05	2046.82	2121.59	2200.92	1.51
0.1	2068.42	2171.38	2284.02	1.56
0.15	2075.24	2185.97	2307.81	1.62
0.2	2080.97	2197.69	2325.86	1.70
0.25	2085.74	2207.26	2340.33	1.62

a suboptimal solution is obtained as one expects. For our model, the improvement in the convergence of Algorithm 2 compared to Algorithm 1 can be numerically demonstrated, while the regularization numerically does not show any improvement when the suboptimality is acceptable.

Remark 3 (*Communication Overhead*)**.** Compared to the standard ADMM, the acceleration variant, as aforementioned, requires the restarting step to ensure convergence for the generic convex problem. Fortunately, this restarting only additionally communicates a scalar between the ath MG and the ADN to determine whether the acceleration operations (16g)–(16j) are activated.

5. Numerical results

Numerical experiments were performed by applying the algorithm to the modified IEEE 69-bus distribution system [54] with four MGs located at nodes 27, 46, 50, and 65. The voltage tolerance is set as [0.95 1.05] p.u. The day-ahead electricity price, the operating characteristics of controllable DGs and ESSs, the day-ahead output of PVs and WTs, and other detailed parameters can be found at [55]. Variation ranges of renewable energy are considered as 20%, which means that the positive/negative deviations of PV and WT power in all MGs are 20% of their forecast values. The scheduling period is one day with an interval of 1 h. Thus there are 24 uncertain WT power forecasts and 24 uncertain PV power forecasts, which means that the budget of uncertainty is between 0 and 48. The initial values of coupling variables and multipliers are all set to 0. To simplify the analysis, the uncertainty budgets of each MG are assumed to be the same. The case study is implemented in Matlab R2016a on an Intel Core i7-8700, 3.2 GHz, 16 GB RAM computer and solved by `Gurobi 9.0`.

5.1. Comparison of different variation ranges

Three different robust cases with different variation ranges for PVs and WTs are considered here: Case 1 (10%), Case 2 (20%), and Case 3 (30%). To simplify the analysis, the uncertainty budgets of each MG are assumed to be the same. Table 1 illustrates the total operation costs and computation time with varying uncertainty budgets. Note that only the solver time is selected for comparison. The following observations can be obtained:

(1) For $\kappa = 0$, the operation costs of the three cases are identical. This is because when the uncertainty budget is zero, no uncertainties can deviate from their forecasts. Thus, $\kappa = 0$ is the traditional deterministic operation model.

(2) For a specific variation range, increasing κ makes the solution more robust at the expense of higher operation costs. Different from the decomposition-based robust model, the impact of κ on the objective value is not monotonic. This is because the second-stage problem in the decomposition-based robust model is a bi-level max–min problem, and a single, worst-case scenario will be identified by the second-stage problem. In the LDRs model, a worst-case scenario will be obtained for each constraint of the second-stage problem. Thus, by increasing κ, the robustness of the LDRs model increases and reaches its maximum value more rapidly than the decomposition-based robust model. Hence, after a specific κ, the robustness level and operation costs remain constant since all uncertainties have adopted their worst-case realizations.

(3) To more accurately evaluate the previous observation, the numerical experiment of Table 1 has been performed in Table 2 with a smaller κ step, i.e., 0.05. As κ increases, the total operation costs monotonically increase until $\kappa = 0.25$. In other words, $\kappa = 0.25$ is the point with the maximum robustness level where all uncertainties have adopted their worst-case realizations.

(4) For a specific value of uncertainty budget, the operation costs increase by increasing the variation range. This is because a greater variation range allows the uncertain renewable energies to deviate more from their forecasts, which leads to a worse worst-case realization. That is, the proposed LDRs model becomes immunized against higher variations of the uncertainties but at the expense of higher operation costs.

(5) By aggregating the renewable energy uncertainties, only a one-dimensional random variable needs to be considered rather than a high-dimensional random variable. Therefore, the computation burden does not increase with the number of uncertain sources. Meanwhile, the proposed LDRs model can simultaneously consider the renewable energy curtailment, optimize the adjustable factors of DGs, and utilize the uncertainty budget in a polyhedral uncertainty set, leading to significantly less conservative solutions.

(6) The computation burden of the proposed LDRs-based adjustable robust operation model is very low, which facilitates its application in real applications.

5.2. Convergence performance and solution quality

The proposed fast ADMM algorithm is compared with its standard counterpart to demonstrate its convergence performance. Taking hour 4 in Case 2 as an example and assuming that the uncertainty budgets of MGs are all 0.2, the iteration processes of the fast ADMM and standard ADMM on the tie-line power and the total operation cost are depicted in Fig. 2 and Fig. 3, respectively. The convergence of the maximum primal and dual residue over the scheduling cycle is shown in Fig. 4. The fast ADMM and standard ADMM algorithms converge after 35 and 53 iterations, with all the primal and dual residues smaller than the thresholds. As expected, the proposed fast ADMM algorithm takes fewer iterations and less time to converge. It can be concluded that the proposed fast ADMM algorithm with predictor–corrector type acceleration step can improve the computation efficiency of decentralized optimization.

The fast ADMM and standard ADMM algorithms are compared with the centralized method to demonstrate comparable solution quality, summarized in Table 3. The converged operation cost found by the fast and standard ADMM is nearly the same as

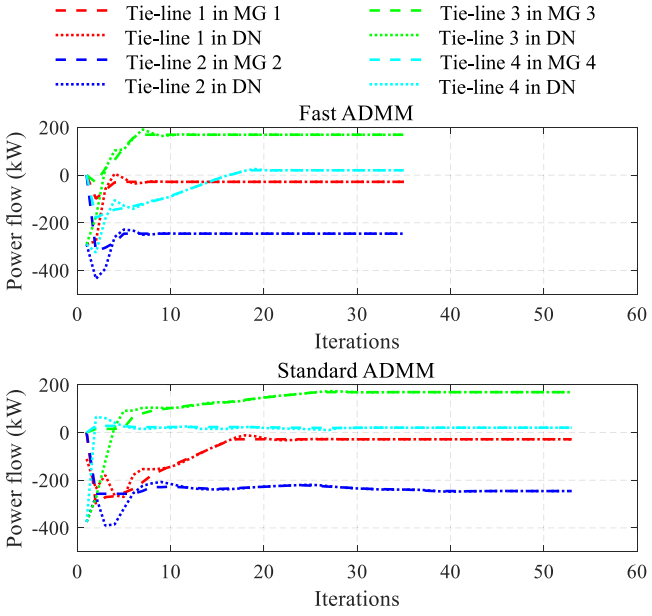

Fig. 2. Convergence of tie-line power flow.

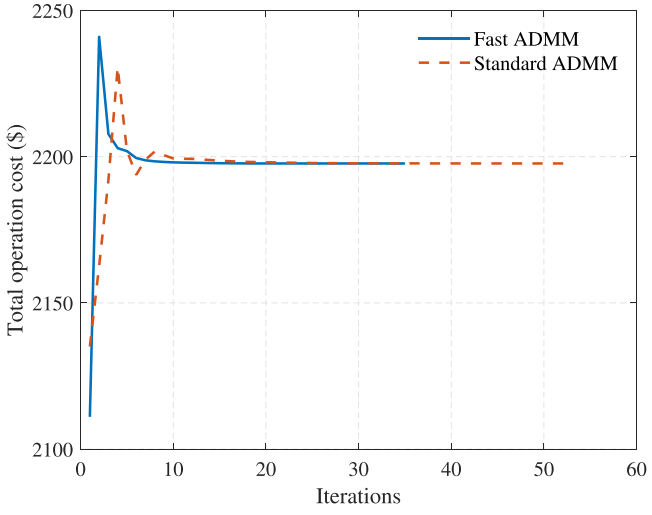

Fig. 3. Convergence of total operation cost.

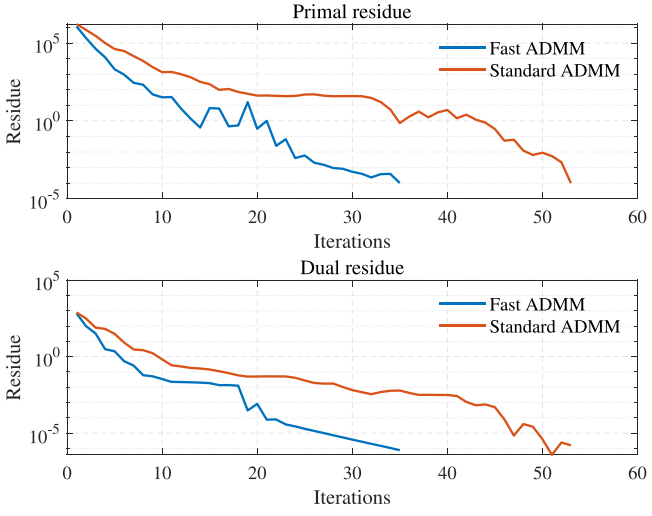

Fig. 4. Convergence of maximum primal and dual residue.

Table 3
Comparison of different algorithms.

Algorithm	Iterations	Total operation cost ($)	Solution gap	Computation time (s)
Centralized	–	2197.69	–	1.70
Standard ADMM	53	2197.70	0.0005%	4.78
Fast ADMM	35	2197.70	0.0005%	2.86

the centralized method. The solution gaps for fast and standard ADMM are all 0.0005%, which is fairly small. The conventional centralized scheme needs a single central super operate entity to control the entire system. However, complete proprietary data of each MG and ADN may not be available, and the area information privacy and operating independence cannot be ensured. In a decentralized manner, only a limited set of information is shared. As a result, communication burdens, which usually account for more processing time in practice, are alleviated, and information privacy is preserved. Compared to the centralized framework, the proposed decentralized method is, thus, potentially more efficient on computation w.r.t the size of the problem that can be addressed and on communication w.r.t the size of information exchanged between neighbors. With the growth in the subsystem scale, the centralized model is difficult to deploy as different subsystems in the multi-microgrids distribution system generally correspond to different operators. Moreover, the proposed LDRs model can also reduce the computation burden of each fast ADMM iteration and guarantee the convergence of the fast ADMM algorithm, and can be easily applied to decentralized optimization.

Although the computing times of the two ADMM algorithms are higher than the centralized model. However, the proposed fast ADMM-based decentralized scheme is not intended to compete with the centralized scheme in computing speed, but to achieve area decomposition aiming for operating autonomy and data privacy. In real applications, subproblems can be simultaneously implemented by local computers in parallel. For both decentralized schemes, the solution gap should asymptotically approach zero. However, for many engineering applications, only a mild level of accuracy is needed. Therefore the computational efficiency of the fast ADMM algorithm will be improved in real applications.

6. Conclusions

Effectively coordinating an active distribution network and multi-microgrids can significantly improve the penetration rate of renewable energy and provide powerful support for the distribution system. This paper proposes a fully decentralized adjustable robust operation framework for an active distribution system with multi-microgrids. The decomposed microgrid operation problem is formulated as a linear decision rules-based two-stage adjustable robust model that includes both “here-and-now” and “wait-and-see” decisions. The linear decision rules approach is utilized to recast the two-stage adjustable robust model into a computationally tractable solution that can be solved directly without decomposition, reducing the computation burden of decentralized optimization. Then, a tailored fast ADMM algorithm with a predictor–corrector type acceleration step is developed to improve the convergence rate of decentralized optimization. The fully decentralized scheme can be solved in a parallel manner, achieving the synergistic yet independent operation of multiple entities.

CRediT authorship contribution statement

Xiao Chen: Conceptualization, Methodology, Software, Investigation, Data Curation, Funding acquisition. **Junyi Zhai:** Software, Investigation, Data Curation, Funding acquisition, Writing – original draft. **Yuning Jiang:** Methodology, Validation, Writing – review & editing, Writing – original draft. **Chenyixuan Ni:** Formal analysis, Writing – review & editing. **Sheng Wang:** Writing – review & editing. **Philippe Nimmegeers:** Validation, Writing – review & editing.

Declaration of competing interest

The authors declare that they have no known competing financial interests or personal relationships that could have appeared to influence the work reported in this paper.

Data availability

Data will be made available on request.

Appendix. Extended formulation of LDRs-based microgrid adjustable robust operation model

In this section, we follow the steps in Section 3 to derive an LDRs-based microgrid adjustable robust operation model, which can simultaneously consider the renewable energy curtailment, optimize the adjustable factors of controllable DGs, and utilize the budget of uncertainty in a polyhedral uncertainty set to reduce solution conservatism.

The uncertainties pertaining to PV and WT power in each MG (omit the microgrid subscript) are modeled through bounded intervals within a polyhedral uncertainty set.

$$\mathcal{U}=\left\{\begin{array}{ll}\tilde{P}_t^W=\overline{P}_t^W+P_t^{W+}-P_t^{W-},\ t\in\mathcal{T} & \\ \tilde{P}_t^P=\overline{P}_t^P+P_t^{P+}-P_t^{P-},\ t\in\mathcal{T} & \\ 0\le P_t^{W+}\le\hat{P}_t^W,\ t\in\mathcal{T} & \mid\lambda_t^{*+}\\ 0\le P_t^{W-}\le\hat{P}_t^W,\ t\in\mathcal{T} & \mid\lambda_t^{*-}\\ 0\le P_t^{P+}\le\hat{P}_t^P,\ t\in\mathcal{T} & \mid\gamma_t^{*+}\\ 0\le P_t^{P-}\le\hat{P}_t^P,\ t\in\mathcal{T} & \mid\gamma_t^{*-}\\ \sum\limits_{t\in\mathcal{T}}\left(\dfrac{P_t^{W+}}{\hat{P}_t^W}+\dfrac{P_t^{W-}}{\hat{P}_t^W}+\dfrac{P_t^{P+}}{\hat{P}_t^P}+\dfrac{P_t^{P-}}{\hat{P}_t^P}\right)\le\kappa & \mid\mu^*\end{array}\right\}\tag{A.1}$$

where λ_t^{*+}, λ_t^{*-}, γ_t^{*+}, γ_t^{*-}, and μ^* represent the dual variables associated with the constraints of the above polyhedral uncertainty set. In the following, the wild-char superscript * is substituted by $B(r)$, $B(l)$, $W(r)$, $W(l)$, $P(r)$, $P(l)$, $C(r)$, $C(l)$, $D(r)$, $D(l)$, $E(r)$, and $E(l)$ in (A.3), (A.4), (A.5), (A.6), (A.7), (A.8), (A.9), (A.10), (A.11), (A.12), (A.13), and (A.14), respectively. These superscripts are characters only used to discriminate the dual variables. This uncertainty set is the extended form of (7) in the compact representation. The size of the uncertainty set $\mathcal{U}$ can be controlled by changing the variation ranges ($\hat{P}_t^W$, $\hat{P}_t^P$) and the budget of uncertainty κ. By increasing the variation ranges or increasing κ, the size of $\mathcal{U}$ increases, which leads to a more robust solution. The choice of κ aims at adjusting the conservativeness of the robust solution. Specifically, choosing $\kappa=0$ leads to the deterministic representation since uncertainties cannot deviate from their forecast values. However, choosing $\kappa>0$ leads to robust representation in which uncertainties can deviate from their forecast values.

To derive a tractable form incorporating the uncertain renewable energy, the following LDRs as a function of the uncertain renewable energy given in (A.1) are considered, which are the extended form of (9). These functions take real-time realizations of the available WT and PV as input and output WT, PV, and ESS actions that keep the negotiated tie-line power constant.

$$P_t^C=P_t^{N,C}+P_t^{A1,C}P_t^{W+}+P_t^{A2,C}P_t^{W-}+P_t^{A3,C}P_t^{P+}+P_t^{A4,C}P_t^{P-},\tag{A.2a}$$

$$P_t^D=P_t^{N,D}+P_t^{A1,D}P_t^{W+}+P_t^{A2,D}P_t^{W-}+P_t^{A3,D}P_t^{P+}+P_t^{A4,D}P_t^{P-},\tag{A.2b}$$

$$P_t^W=P_t^{N,W}+P_t^{A1,W}P_t^{W+}+P_t^{A2,W}P_t^{W-}+P_t^{A3,W}P_t^{P+}+P_t^{A4,W}P_t^{P-},\tag{A.2c}$$

$$P_t^P=P_t^{N,P}+P_t^{A1,P}P_t^{W+}+P_t^{A2,P}P_t^{W-}+P_t^{A3,P}P_t^{P+}+P_t^{A4,P}P_t^{P-},\tag{A.2d}$$

where the non-adjustable terms ($P_t^{N,C}$, $P_t^{N,D}$, $P_t^{N,W}$, $P_t^{N,P}$) represent the first stage "here-and-now" decisions, while the remaining adjustable terms ($P_t^{A1,C}$, $P_t^{A2,C}$, $P_t^{A3,C}$, $P_t^{A4,C}$, $P_t^{A1,D}$, $P_t^{A2,D}$, $P_t^{A3,D}$, $P_t^{A4,D}$, $P_t^{A1,W}$, $P_t^{A2,W}$, $P_t^{A3,W}$, $P_t^{A4,W}$, $P_t^{A1,P}$, $P_t^{A2,P}$, $P_t^{A3,P}$, $P_t^{A4,P}$) represent the second stage "wait-and-see" recourse decisions, which can be seen as the adjustable factors of controllable DGs. As it is seen, P_t^W and P_t^P have also been used in these auxiliary variables (i.e., $P_t^{N,W}$, $P_t^{A1,W}$, $P_t^{A2,W}$, $P_t^{A3,W}$, $P_t^{A4,W}$ and $P_t^{N,P}$, $P_t^{A1,P}$, $P_t^{A2,P}$, $P_t^{A3,P}$, $P_t^{A4,P}$ to indicate that these auxiliary variables are associated with the decision variables P_t^W and P_t^P. However, these auxiliary variables are sufficiently discriminated from decision variables P_t^W and P_t^P using superscripts N, A1, A2, A3, and A4. In (A.2a)-(A.2d), the unit of auxiliary variables with superscript N is kW, and the auxiliary variables with superscripts A1, A2, A3, and A4 are dimensionless.

The LDRs-based microgrid adjustable robust operation model can be obtained from the deterministic operation model (3) by replacing the certain WT and PV forecasts with their uncertain values and using the above-mentioned LDRs. Without loss of generality, we respectively replace the power balance equality constraint (3b) and the ESS energy balance equality constraint (3h) with two inequality constraints. Then using the duality theory, the tractable formulation of the power balance equality constraint and the ESS energy balance equality constraint, which is feasible for any realization of the uncertainties belonging to the polyhedral uncertainty set, can be written into the following (A.3), (A.4) and (A.13), (A.14). In the following, (3) can be reformulated by first substituting in (A.2), and then replacing the max operator over the uncertainty set with its dual equivalent. The tractable formulation, which is feasible for any realization of the uncertainties belonging to the polyhedral uncertainty set, can be written using the duality theory as follows:

$$\min\quad\sum_{t\in\mathcal{T}}\left(c^C P_t^{N,C}+c^D P_t^{N,D}\right)\tag{A.3a}$$

subject to

$$\begin{aligned}&P_t^{N,W}+P_t^{N,P}+P_t^{MG}+P_t^{N,D}-P_t^{N,C}+4\kappa\mu^B(r)+\\&\hat{P}_t^W\lambda_t^{B(r)+}+\hat{P}_t^W\lambda_t^{B(r)-}+\hat{P}_t^P\gamma_t^{B(r)+}+\hat{P}_t^P\gamma_t^{B(r)-}\le P_t^L\end{aligned}\tag{A.3b}$$

$$\hat{P}_t^W\lambda_t^{B(r)+}+\mu^{B(r)}\ge\hat{P}_t^W\left(P_t^{A1,D}-P_t^{A1,C}+P_t^{A1,W}+P_t^{A1,P}\right)\tag{A.3c}$$

$$\hat{P}_t^W\lambda_t^{B(r)-}+\mu^{B(r)}\ge\hat{P}_t^W\left(P_t^{A2,D}-P_t^{A2,C}+P_t^{A2,W}+P_t^{A2,P}\right)\tag{A.3d}$$

$$\hat{P}_t^P\gamma_t^{B(r)+}+\mu^{B(r)}\ge\hat{P}_t^P\left(P_t^{A3,D}-P_t^{A3,C}+P_t^{A3,W}+P_t^{A3,P}\right)\tag{A.3e}$$

$$\hat{P}_t^P\gamma_t^{B(r)-}+\mu^{B(r)}\ge\hat{P}_t^P\left(P_t^{A4,D}-P_t^{A4,C}+P_t^{A4,W}+P_t^{A4,P}\right)\tag{A.3f}$$

$$\lambda_t^{B(r)+}\ge0,\ \lambda_t^{B(r)-}\ge0,\ \gamma_t^{B(r)+}\ge0,\ \gamma_t^{B(r)-}\ge0,\ \mu^{B(r)}\ge0\tag{A.3g}$$

and

$$-P_t^{N,W} - P_t^{N,P} - P_t^{MG} - P_t^{N,D} + P_t^{N,C} + 4\kappa\mu^{B}(l) + \hat{P}_t^W\lambda_t^{B(l)+} + \hat{P}_t^W\lambda_t^{B(l)-} + \hat{P}_t^P\gamma_t^{B(l)+} + \hat{P}_t^P\gamma_t^{B(l)-} \le P_t^L \quad (A.4a)$$

$$\hat{P}_t^W\lambda_t^{B(l)+} + \mu^{B(l)} \ge \hat{P}_t^W\left(P_t^{A1,C} - P_t^{A1,D} - P_t^{A1,W} - P_t^{A1,P}\right) \quad (A.4b)$$

$$\hat{P}_t^W\lambda_t^{B(l)-} + \mu^{B(l)} \ge \hat{P}_t^W\left(P_t^{A2,C} - P_t^{A2,D} - P_t^{A2,W} - P_t^{A2,P}\right) \quad (A.4c)$$

$$\hat{P}_t^P\gamma_t^{B(l)+} + \mu^{B(l)} \ge \hat{P}_t^P\left(P_t^{A3,C} - P_t^{A3,D} - P_t^{A3,W} - P_t^{A3,P}\right) \quad (A.4d)$$

$$\hat{P}_t^P\gamma_t^{B(l)-} + \mu^{B(l)} \ge \hat{P}_t^P\left(P_t^{A4,C} - P_t^{A4,D} - P_t^{A4,W} - P_t^{A4,P}\right) \quad (A.4e)$$

$$\lambda_t^{B(l)+} \ge 0, \lambda_t^{B(l)-} \ge 0, \gamma_t^{B(l)+} \ge 0, \gamma_t^{B(l)-} \ge 0, \mu^{B(l)} \ge 0 \quad (A.4f)$$

and

$$\hat{P}_t^W\lambda_t^{W(r)+} + \hat{P}_t^W\lambda_t^{W(r)-} + \hat{P}_t^P\lambda_t^{W(r)+} + \hat{P}_t^P\gamma_t^{W(r)-} + 4\kappa\mu^{W(r)} \le \bar{P}^W - P_t^{N,W} \quad (A.5a)$$

$$\hat{P}_t^W\lambda_t^{W(r)+} + \mu^{W(r)} \ge \hat{P}_t^W\left(P_t^{A1,W} - 1\right) \quad (A.5b)$$

$$\hat{P}_t^W\lambda_t^{W(r)-} + \mu^{W(r)} \ge \hat{P}_t^W\left(P_t^{A2,W} + 1\right) \quad (A.5c)$$

$$\hat{P}_t^P\gamma_t^{W(r)+} + \mu^{W(r)} \ge \hat{P}_t^P P_t^{A3,W} \quad (A.5d)$$

$$\hat{P}_t^P\gamma_t^{W(r)-} + \mu^{W(r)} \ge \hat{P}_t^P P_t^{A4,W} \quad (A.5e)$$

$$\lambda_t^{W(r)+} \ge 0, \lambda_t^{W(r)-} \ge 0, \gamma_t^{W(r)+} \ge 0, \gamma_t^{W(r)-} \ge 0, \mu^{W(r)} \ge 0 \quad (A.5f)$$

and

$$\hat{P}_t^W\lambda_t^{W(l)+} + \hat{P}_t^W\lambda_t^{W(l)-} + \hat{P}_t^P\lambda_t^{W(l)+} + \hat{P}_t^P\gamma_t^{W(l)-} + 4\kappa\mu^{W(l)} \le P_t^{N,W} \quad (A.6a)$$

$$\hat{P}_t^W\lambda_t^{W(l)+} + \mu^{W(l)} \ge -\hat{P}_t^W P_t^{A1,W} \quad (A.6b)$$

$$\hat{P}_t^W\lambda_t^{W(l)-} + \mu^{W(l)} \ge -\hat{P}_t^W P_t^{A2,W} \quad (A.6c)$$

$$\hat{P}_t^P\gamma_t^{W(l)+} + \mu^{W(l)} \ge -\hat{P}_t^P P_t^{A3,W} \quad (A.6d)$$

$$\hat{P}_t^P\gamma_t^{W(l)-} + \mu^{W(l)} \ge -\hat{P}_t^P P_t^{A4,W} \quad (A.6e)$$

$$\lambda_t^{W(l)+} \ge 0, \lambda_t^{W(l)-} \ge 0, \gamma_t^{W(l)+} \ge 0, \gamma_t^{W(l)-} \ge 0, \mu^{W(l)} \ge 0 \quad (A.6f)$$

and

$$\hat{P}_t^P\lambda_t^{P(r)} + \hat{P}_t^P\lambda_t^{P(r)-} + \hat{P}_t^W\gamma_t^{P(r)+} + \hat{P}_t^W\gamma_t^{P(r)-} + 4\kappa\mu^{P(r)} \le \bar{P}^P - P^{N,P} \quad (A.7a)$$

$$\hat{P}_t^P\lambda_t^{P(r)+} + \mu^{P(r)} \ge \hat{P}_t^P\left(P_t^{A1,P} - 1\right) \quad (A.7b)$$

$$\hat{P}_t^P\lambda_t^{P(r)-} + \mu^{P(r)} \ge \hat{P}_t^P\left(P_t^{A2,P} + 1\right) \quad (A.7c)$$

$$\hat{P}_t^W\gamma_t^{P(r)+} + \mu^{P(r)} \ge \hat{P}_t^W P_t^{A3,P} \quad (A.7d)$$

$$\hat{P}_t^W\gamma_t^{P(r)-} + \mu^{P(r)} \ge \hat{P}^W P_t^{A4,P} \quad (A.7e)$$

$$\lambda_t^{P(r)+} \ge 0, \lambda_t^{P(r)-} \ge 0, \gamma_t^{P(r)+} \ge 0, \gamma_t^{P(r)-} \ge 0, \mu^{P(r)} \ge 0 \quad (A.7f)$$

and

$$\hat{P}_t^P\lambda_t^{P(l)} + \hat{P}_t^P\lambda_t^{P(l)-} + \hat{P}_t^W\gamma_t^{P(l)+} + \hat{P}_t^W\gamma_t^{P(l)-} + 4\kappa\mu^{P(l)} \le P^{N,P} \quad (A.8a)$$

$$\hat{P}_t^P\lambda_t^{P(l)+} + \mu^{P(l)} \ge -\hat{P}_t^P P_t^{A1,P} \quad (A.8b)$$

$$\hat{P}_t^P\lambda_t^{P(l)-} + \mu^{P(l)} \ge -\hat{P}_t^P P_t^{A2,P} \quad (A.8c)$$

$$\hat{P}_t^W\gamma_t^{P(l)+} + \mu^{P(l)} \ge -\hat{P}_t^W P_t^{A3,P} \quad (A.8d)$$

$$\hat{P}_t^W\gamma_t^{P(l)-} + \mu^{P(l)} \ge -\hat{P}^W P_t^{A4,P} \quad (A.8e)$$

$$\lambda_t^{P(l)+} \ge 0, \lambda_t^{P(l)-} \ge 0, \gamma_t^{P(l)+} \ge 0, \gamma_t^{P(l)-} \ge 0, \mu^{P(l)} \ge 0 \quad (A.8f)$$

and

$$\hat{P}_t^W\lambda_t^{C(r)+} + \hat{P}_t^W\lambda_t^{C(r)-} + \hat{P}_t^P\gamma_t^{C(r)+} + \hat{P}_t^P\gamma_t^{C(r)-} + 4\kappa\mu^{C(r)} \le \bar{P}^C - P_t^{N,C} \quad (A.9a)$$

$$\hat{P}_t^W\lambda_t^{C(r)+} + \mu^{C(r)} \ge \hat{P}_t^W P_t^{A1,C} \quad (A.9b)$$

$$\hat{P}_t^W\lambda_t^{C(r)-} + \mu^{C(r)} \ge \hat{P}_t^W P_t^{A2,C} \quad (A.9c)$$

$$\hat{P}_t^P\gamma_t^{C(r)+} + \mu^{C(r)} \ge \hat{P}_t^P P_t^{A3,C} \quad (A.9d)$$

$$\hat{P}_t^P\gamma_t^{C(r)-} + \mu^{C(r)} \ge \hat{P}_t^P P_t^{A4,C} \quad (A.9e)$$

$$\lambda_t^{C(r)+} \ge 0, \lambda_t^{C(r)-} \ge 0, \gamma_t^{C(r)+} \ge 0, \gamma_t^{C(r)-} \ge 0, \mu^{C(r)} \ge 0 \quad (A.9f)$$

and

$$\hat{P}_t^W\lambda_t^{C(l)+} + \hat{P}_t^W\lambda_t^{C(l)-} + \hat{P}_t^P\gamma_t^{C(l)+} + \hat{P}_t^P\gamma_t^{C(l)-} + 4\kappa\mu^{C(l)} \le P_t^{N,C} \quad (A.10a)$$

$$\hat{P}_t^W\lambda_t^{C(l)+} + \mu^{C(l)} \ge -\hat{P}_t^W P_t^{A1,C} \quad (A.10b)$$

$$\hat{P}_t^W\lambda_t^{C(l)-} + \mu^{C(l)} \ge -\hat{P}_t^W P_t^{A2,C} \quad (A.10c)$$

$$\hat{P}_t^P\gamma_t^{C(l)+} + \mu^{C(l)} \ge -\hat{P}_t^P P_t^{A3,C} \quad (A.10d)$$

$$\hat{P}_t^P\gamma_t^{C(l)-} + \mu^{C(l)} \ge -\hat{P}_t^P P_t^{A4,C} \quad (A.10e)$$

$$\lambda_t^{C(l)+} \ge 0, \lambda_t^{C(l)-} \ge 0, \gamma_t^{C(l)+} \ge 0, \gamma_t^{C(l)-} \ge 0, \mu^{C(l)} \ge 0 \quad (A.10f)$$

and

$$\hat{P}_t^W\lambda_t^{D(r)+} + \hat{P}_t^W\lambda_t^{D(r)-} + \hat{P}_t^P\gamma_t^{D(r)+} + \hat{P}_t^P\gamma_t^{D(r)-} + 4\kappa\mu^{D(r)} \le \bar{P}^D - P_t^{N,D} \quad (A.11a)$$

$$\hat{P}_t^W\lambda_t^{D(r)+} + \mu^{D(r)} \ge \hat{P}_t^W P_t^{A1,D} \quad (A.11b)$$

$$\hat{P}_t^W\lambda_t^{D(r)-} + \mu^{D(r)} \ge \hat{P}_t^W P_t^{A2,D} \quad (A.11c)$$

$$\hat{P}_t^P\gamma_t^{D(r)+} + \mu^{D(r)} \ge \hat{P}_t^P P_t^{A3,D} \quad (A.11d)$$

$$\hat{P}_t^P\gamma_t^{D(r)-} + \mu^{D(r)} \ge \hat{P}_t^P P_t^{A4,D} \quad (A.11e)$$

$$\lambda_t^{D(r)+} \ge 0, \lambda_t^{D(r)-} \ge 0, \gamma_t^{D(r)+} \ge 0, \gamma_t^{D(r)-} \ge 0, \mu^{D(r)} \ge 0 \quad (A.11f)$$

and

$$\hat{P}_t^W\lambda_t^{D(l)+} + \hat{P}_t^W\lambda_t^{D(l)-} + \hat{P}_t^P\gamma_t^{D(l)+} + \hat{P}_t^P\gamma_t^{D(l)-} + 4\kappa\mu^{D(l)} \le P_t^{N,D} \quad (A.12a)$$

$$\hat{P}_t^W\lambda_t^{D(l)+} + \mu^{D(l)} \ge -\hat{P}_t^W P_t^{A1,D} \quad (A.12b)$$

$$\hat{P}_t^W\lambda_t^{D(l)-} + \mu^{D(l)} \ge -\hat{P}_t^W P_t^{A2,D} \quad (A.12c)$$

$$\hat{P}_t^P\gamma_t^{D(l)+} + \mu^{D(l)} \ge -\hat{P}_t^P P_t^{A3,D} \quad (A.12d)$$

$$\hat{P}_t^P\gamma_t^{D(l)-} + \mu^{D(l)} \ge -\hat{P}_t^P P_t^{A4,D} \quad (A.12e)$$

$$\lambda_t^{D(l)+} \ge 0, \lambda_t^{D(l)-} \ge 0, \gamma_t^{D(l)+} \ge 0, \gamma_t^{D(l)-} \ge 0, \mu^{D(l)} \ge 0 \quad (A.12f)$$

and

$$P_t^{N,C}\eta^C - P_t^{N,D}/\eta^D + \hat{P}_t^W\lambda_t^{E(r)+} + \hat{P}_t^W\lambda_t^{E(r)-} + \hat{P}_t^P\gamma_t^{E(r)+} + \hat{P}_t^P\gamma_t^{E(r)-} + 4\kappa\mu^{E(r)} \le E_t - E_{t-1} \quad (A.13a)$$

$$\hat{P}_t^W\lambda_t^{E(r)+} + \mu^{E(r)} \ge \hat{P}_t^W\left(P_t^{A1,C}\eta^C - P_t^{A1,D}/\eta^D\right) \quad (A.13b)$$

$$\hat{P}_t^W\lambda_t^{E(r)-} + \mu^{E(r)} \ge \hat{P}_t^W\left(P_t^{A2,C}\eta^C - P_t^{A2,D}/\eta^D\right) \quad (A.13c)$$

$$\hat{P}_t^P\gamma_t^{E+(r)} + \mu^{E(r)} \ge \hat{P}_t^P\left(P_t^{A3,C}\eta^C - P_t^{A3,D}/\eta^D\right) \quad (A.13d)$$

$$\hat{P}_t^P\gamma_t^{E(r)-} + \mu^{E(r)} \ge \hat{P}_t^P\left(P_t^{A4,C}\eta^C - P_t^{A4,D}/\eta^D\right) \quad (A.13e)$$

$$\lambda_t^{E(r)+} \ge 0, \lambda_t^{E(r)-} \ge 0, \gamma_t^{E(r)+} \ge 0, \gamma_t^{E(r)-} \ge 0, \mu^{E(r)} \ge 0 \quad (A.13f)$$

and

$$-P_t^{N,C}\eta^C + P_t^{N,D}/\eta^D + \hat{P}_t^W\lambda_t^{E(l)+} + \hat{P}_t^W\lambda_t^{E(l)-} + \hat{P}_t^P\gamma_t^{E(l)+} + \hat{P}_t^P\gamma_t^{E(l)-} + 4\kappa\mu^{E(l)} \le E_{t-1} - E_t \quad (A.14a)$$

$$\hat{P}_t^W\lambda_t^{E(l)+} + \mu^{E(l)} \ge \hat{P}_t^W\left(P_t^{A1,D}/\eta^D - P_t^{A1,C}\eta^C\right) \quad (A.14b)$$

$$\hat{P}_t^W \lambda_t^{E(I)-} + \mu^{E(I)} \geq \hat{P}_t^W \left(P_t^{A2,D}/\eta^D - P_t^{A2,C}\eta^C \right) \quad \text{(A.14c)}$$

$$\hat{P}_t^P \gamma_t^{E(I)+} + \mu^{E(I)} \geq \hat{P}_t^P \left(P_t^{A3,D}/\eta^D - P_t^{A3,C}\eta^C \right) \quad \text{(A.14d)}$$

$$\hat{P}_t^P \gamma_t^{E(I)-} + \mu^{E(I)} \geq \hat{P}_t^P \left(P_t^{A4,D}/\eta^D - P_t^{A4,C}\eta^C \right) \quad \text{(A.14e)}$$

$$\lambda_t^{E(I)+} \geq 0, \lambda_t^{E(I)-} \geq 0, \gamma_t^{E(I)+} \geq 0, \gamma_t^{E(I)-} \geq 0, \mu^{E(I)} \geq 0. \quad \text{(A.14f)}$$

and

(3c), (3i), (3j) (A.15)

References

[1] S. Amir Mansouri, M.S. Javadi, A. Ahmarinejad, E. Nematbakhsh, A. Zare, J.P. Catalão, A coordinated energy management framework for industrial, residential and commercial energy hubs considering demand response programs, Sustain. Energy Technol. Assess. 47 (2021) 101376.

[2] J. Zhai, S. Wang, L. Guo, Y. Jiang, Z. Kang, C.N. Jones, Data-driven distributionally robust joint chance-constrained energy management for multi-energy microgrid, Appl. Energy 326 (2022) 119939.

[3] S. Wang, H. Hui, Y. Ding, C. Ye, M. Zheng, Operational reliability evaluation of urban multi-energy systems with equivalent energy storage, IEEE Trans. Ind. Appl. (2022).

[4] P. Wu, W. Huang, N. Tai, S. Liang, A novel design of architecture and control for multiple microgrids with hybrid AC/DC connection, Appl. Energy 210 (2018) 1002–1016.

[5] H. Kiani, K. Hesami, A. Azarhooshang, S. Pirouzi, S. Safaee, Adaptive robust operation of the active distribution network including renewable and flexible sources, Sustain. Energy, Grids Netw. 26 (2021) 100476.

[6] Z. Li, Y. Xu, Optimal coordinated energy dispatch of a multi-energy microgrid in grid-connected and islanded modes, Appl. Energy 210 (2018) 974–986.

[7] M. Li, X. Zhang, G. Li, C. Jiang, A feasibility study of microgrids for reducing energy use and GHG emissions in an industrial application, Appl. Energy 176 (2016) 138–148.

[8] S. Wang, J. Zhai, H. Hui, Optimal energy flow in integrated electricity and gas systems with injection of alternative gas, IEEE Trans. Sustain. Energy (2023).

[9] L. Yan, X. Chen, Y. Chen, J. Wen, A cooperative charging control strategy for electric vehicles based on multiagent deep reinforcement learning, IEEE Trans. Ind. Inform. 18 (12) (2022) 8765–8775.

[10] Y. Du, Z. Wang, G. Liu, X. Chen, H. Yuan, Y. Wei, F. Li, A cooperative game approach for coordinating multi-microgrid operation within distribution systems, Appl. Energy 222 (2018) 383–395.

[11] A. Ouammi, H. Dagdougui, L. Dessaint, R. Sacile, Coordinated model predictive-based power flows control in a cooperative network of smart microgrids, IEEE Trans. Smart Grid 6 (5) (2015) 2233–2244.

[12] B. Zhang, Q. Li, L. Wang, W. Feng, Robust optimization for energy transactions in multi-microgrids under uncertainty, Appl. Energy 217 (2018) 346–360.

[13] T. Sattarpour, S. Golshannavaz, D. Nazarpour, P. Siano, A multi-stage linearized interactive operation model of smart distribution grid with residential microgrids, Int. J. Electr. Power Energy Syst. 108 (2019) 456–471.

[14] Z. Li, X. Yan, Optimal coordinated energy dispatch of a multi-energy microgrid in grid-connected and islanded modes - ScienceDirect, Appl. Energy 210 (2018) 974–986.

[15] A. Zidan, H.A. Gabbar, A. Eldessouky, Optimal planning of combined heat and power systems within microgrids, Energy 93 (2015) 235–244.

[16] D. Zhang, S. Evangelisti, P. Lettieri, L.G. Papageorgiou, Optimal design of CHP-based microgrids: Multiobjective optimisation and life cycle assessment, Energy 85 (2015) 181–193.

[17] M. Lotfi, G.J. Osório, M.S. Javadi, M.S. El Moursi, C. Monteiro, J.P. Catalão, A fully decentralized machine learning algorithm for optimal power flow with cooperative information exchange, Int. J. Electr. Power Energy Syst. 139 (2022) 107990.

[18] J. Zhai, X. Dai, Y. Jiang, Y. Xue, V. Hagenmeyer, C.N. Jones, X.-P. Zhang, Distributed optimal power flow for VSC-MTDC meshed AC/DC grids using ALADIN, IEEE Trans. Power Syst. 37 (6) (2022) 4861–4873.

[19] C. Feng, B. Liang, Z. Li, W. Liu, F. Wen, Peer-to-peer energy trading under network constraints based on generalized fast dual ascent, IEEE Trans. Smart Grid (2022) 1.

[20] Z. Chen, C. Guo, S. Dong, Y. Ding, H. Mao, Distributed robust dynamic economic dispatch of integrated transmission and distribution systems, IEEE Trans. Ind. Appl. (2021) 1.

[21] J. Zhai, Y. Jiang, Y. Shi, C.N. Jones, X.-P. Zhang, Distributionally robust joint chance-constrained dispatch for integrated transmission-distribution systems via distributed optimization, IEEE Trans. Smart Grid 13 (3) (2022) 2132–2147.

[22] J. Zhai, Y. Jiang, J. Li, C. Jones, X.-P. Zhang, Distributed adjustable robust optimal power-gas flow considering wind power uncertainty, Int. J. Electr. Power Energy Syst. 139 (2022).

[23] J. Zhai, Y. Jiang, X. Chen, J. Li, C.N. Jones, X.-P. Zhang, Asynchronous decentralized adjustable robust operation for multi-area integrated electricity–gas systems considering wind power uncertainty, Int. J. Electr. Power Energy Syst. 147 (2023) 108882.

[24] M.S. Javadi, A. Esmaeel Nezhad, A.R. Jordehi, M. Gough, S.F. Santos, J.P. Catalão, Transactive energy framework in multi-carrier energy hubs: A fully decentralized model, Energy 238 (2022) 121717.

[25] M. Zhou, J. Zhai, G. Li, J. Ren, Distributed dispatch approach for bulk AC/DC hybrid systems with high wind power penetration, IEEE Trans. Power Syst. 33 (3) (2018) 3325–3336.

[26] J. Zhai, M. Zhou, J. Li, X. Zhang, G. Li, C. Ni, W. Zhang, Hierarchical and robust scheduling approach for VSC-MTDC meshed AC/DC grid with high share of wind power, IEEE Trans. Power Syst. (2020) 1.

[27] C. Lin, W. Wu, B. Zhang, Y. Sun, Decentralized solution for combined heat and power dispatch through benders decomposition, IEEE Trans. Sustain. Energy 8 (4) (2017) 1361–1372.

[28] Z. Li, Q. Guo, H. Sun, J. Wang, Coordinated economic dispatch of coupled transmission and distribution systems using heterogeneous decomposition, IEEE Trans. Power Syst. 31 (6) (2016) 4817–4830.

[29] J. Wang, H. Zhong, Z. Yang, X. Lai, Q. Xia, C. Kang, Incentive mechanism for clearing energy and reserve markets in multi-area power systems, IEEE Trans. Sustain. Energy 11 (4) (2020) 2470–2482.

[30] M.S. Javadi, A. Anvari-Moghaddam, J.M. Guerrero, Robust energy hub management using information gap decision theory, in: IECON 2017-43rd Annual Conference of the IEEE Industrial Electronics Society, IEEE, 2017, pp. 410–415.

[31] Z. Wang, B. Chen, J. Wang, M.M. Begovic, C. Chen, Coordinated energy management of networked microgrids in distribution systems, IEEE Trans. Smart Grid 6 (1) (2014) 45–53.

[32] D. Wang, X. Guan, J. Wu, P. Li, P. Zan, H. Xu, Integrated energy exchange scheduling for multimicrogrid system with electric vehicles, IEEE Trans. Smart Grid 7 (4) (2015) 1762–1774.

[33] Z. Li, W. Wu, B. Zeng, M. Shahidehpour, B. Zhang, Decentralized contingency-constrained tie-line scheduling for multi-area power grids, IEEE Trans. Power Syst. 32 (1) (2017) 354–367.

[34] B. Zeng, L. Zhao, Solving two-stage robust optimization problems using a column-and-constraint generation method, Oper. Res. Lett. 41 (5) (2013) 457–461.

[35] C. He, L. Wu, T. Liu, M. Shahidehpour, Robust co-optimization scheduling of electricity and natural gas systems via ADMM, IEEE Trans. Sustain. Energy 8 (2) (2017) 658–670.

[36] D. Bertsimas, E. Litvinov, X.A. Sun, J. Zhao, T. Zheng, Adaptive robust optimization for the security constrained unit commitment problem, IEEE Trans. Power Syst. 28 (1) (2013) 52–63.

[37] Z. Li, W. Wu, B. Zhang, B. Wang, Adjustable robust real-time power dispatch with large-scale wind power integration, IEEE Trans. Sustain. Energy 6 (2) (2015) 357–368.

[38] J. Zhao, T. Zheng, E. Litvinov, Variable resource dispatch through do-not-exceed limit, IEEE Trans. Power Syst. 30 (2) (2015) 820–828.

[39] R.A. Jabr, S. Karaki, J.A. Korbane, Robust multi-period OPF with storage and renewables, IEEE Trans. Power Syst. 30 (5) (2015) 2790–2799.

[40] R.A. Jabr, Adjustable robust OPF with renewable energy sources, IEEE Trans. Power Syst. 28 (4) (2013) 4742–4751.

[41] R. Wang, P. Wang, G. Xiao, A robust optimization approach for energy generation scheduling in microgrids, Energy Convers. Manage. 106 (2015) 597–607.

[42] S.D. Manshadi, M.E. Khodayar, Risk-averse generation maintenance scheduling with microgrid aggregators, IEEE Trans. Smart Grid 9 (6) (2017) 6470–6479.

[43] L. Wang, B. Zhang, Q. Li, W. Song, G. Li, Robust distributed optimization for energy dispatch of multi-stakeholder multiple microgrids under uncertainty, Appl. Energy 255 (2019) 113845.

[44] M. Baran, F.F. Wu, Optimal sizing of capacitors placed on a radial distribution system, IEEE Trans. Power Deliv. 4 (1) (1989) 735–743.

[45] H. Yeh, D.F. Gayme, S.H. Low, Adaptive VAR control for distribution circuits with photovoltaic generators, IEEE Trans. Power Syst. 27 (3) (2012) 1656–1663.

[46] M.S. Javadi, M. Gough, S.A. Mansouri, A. Ahmarinejad, E. Nematbakhsh, S.F. Santos, J.P. Catalão, A two-stage joint operation and planning model for sizing and siting of electrical energy storage devices considering demand response programs, Int. J. Electr. Power Energy Syst. 138 (2022) 107912.
[47] S. Boyd, S.P. Boyd, L. Vandenberghe, Convex Optimization, Cambridge University Press, 2004.
[48] P. Xiong, P. Jirutitijaroen, A linear decision rule approach for robust unit commitment considering wind power generation, in: 2014 Power Systems Computation Conference, IEEE, 2014, pp. 1–7.
[49] Y. Jiang, P. Sauerteig, B. Houska, K. Worthmann, Distributed optimization using ALADIN for MPC in smart grids, IEEE Trans. Control Syst. Technol. 29 (5) (2021) 2142–2152.
[50] Y. Nesterov, et al., Lectures on Convex Optimization, Vol. 137, Springer, 2018.
[51] T. Goldstein, B. O'Donoghue, S. Setzer, R. Baraniuk, Fast alternating direction optimization methods, SIAM J. Imaging Sci. 7 (3) (2014) 1588–1623.
[52] A. Buccini, P. Dell'Acqua, M. Donatelli, A general framework for ADMM acceleration, Numer. Algorithms 85 (3) (2020) 829–848.
[53] J. Su, Y. Jiang, A. Bitlislioglu, C. Jones, B. Houska, Distributed multi-building coordination for demand response, in: IFAC PapersOnLine, 53, (2) 2020, pp. 17113–17118.
[54] J.S. Savier, D. Das, Impact of network reconfiguration on loss allocation of radial distribution systems, IEEE Trans. Power Deliv. 22 (4) (2007) 2473–2480.
[55] https://github.com/JunyiZhai1990/ADN-with-MMG.